

A Novel and Elliptical Lattice Design of Flocking Control for Multi-Agent Ground Vehicles

Gang Wang, Mingzhe Liu, Fengchen Wang, and Yan Chen Member, IEEE

Abstract—Flocking control of multi-agent ground vehicles recently attracted rising attention because of its strength in extending 1D platooning to coordinated 2D movements. However, the uniform interaction ranges and the non-defined orientation of the flocking lattice make flocking control of ground vehicles face some key issues. To achieve cooperative motions of connected and automated vehicles (CAVs), this letter proposed a novel and elliptical lattice to extend the existing flocking theory with a uniform hexagon lattice. The proposed elliptical lattice is designed based on the characteristics of the vehicle heading direction, velocity, minimum safety distance, and lane width to analytically adapt to vehicle driving environments. Moreover, a new flocking control law considering road boundaries' (permanent) repulsive forces is developed to ensure the desired formation at a steady state. Simulation results show that the proposed elliptical lattice of flocking control can be applied to realize cooperative driving of multi-agent CAVs with the desired formation on the road.

Index Terms—Flocking control, flocking lattice, multiagent systems, connected and automated vehicles.

I. INTRODUCTION

TLOCKING, as a collective behavior, has attracted great attention and research interest. To analyze flocking behaviours, three types of agents, namely α -agents, β -agents, and γ -agent(s), are introduced to represent a group of cooperative agents, obstacles, and (virtual) leader(s), respectively [1], [2], [3], [4]. To regulate $\alpha - \alpha$ interactions in motion, control laws are designed to form (quasi) α -lattices, which are typically in the shape of hexagons [2], [5], [6], [7]. Together with control laws for $\alpha - \beta$ interactions (to avoid obstacles) and $\alpha - \gamma$ interactions (to track leader(s)), some well-known flocking rules for α -agents can be achieved, such as flocking centering, collision avoidance, velocity matching, virtual leader navigation, and obstacle avoidance [2], [4], [8], [9].

Recently, flocking control was applied to multi-agent ground vehicles. For example, autonomous driving algorithms using

Manuscript received 16 September 2022; revised 13 November 2022; accepted 6 December 2022. Date of publication 23 December 2022; date of current version 6 January 2023. This work was supported in part by the Office of Naval Research (ONR) under Grant N00014-21-1-2403. Recommended by Senior Editor L. Zhang. (Corresponding author: Yan Chen.)

The authors are with the Polytechnic School, Arizona State University, Mesa, AZ 85212 USA (e-mail: gwang109@asu.edu; mingzhe.liu@asu.edu; fengchen.w@asu.edu; yanchen@asu.edu).

Digital Object Identifier 10.1109/LCSYS.2022.3231628

flocking theory were proposed to perform different driving scenarios [10]. Two improved flocking protocols were introduced to achieve lane-following and braking control [1]. Nonlinear vehicle dynamics [3], [11] and permanent obstacles [12] were investigated for flocking control of connected and automated vehicles (CAVs). These works relied on uniform interaction distances among vehicles (α -agents) without considering the influence of vehicle speeds and orientations on the formed flocking lattice. However, the vehicle's longitudinal speed is usually much larger than the lateral speed, which indicates that the lattice scale in the longitudinal direction should be larger than that in the lateral direction. This common feature of ground vehicle movements needs to be modeled in the application of flocking control, which cannot be represented by the existing uniform hexagon lattice.

To form different longitudinal and lateral inter-vehicle spacing, a flock-like model with additional rules was developed [13]. Specific triangular vehicle formations were proposed via confidence analysis [14] or permission-based strategies [15], while maintenance required lane-changing tasks. For the first time, an adaptive spacing policy was developed by the authors to describe nonuniform flocking movements of ground vehicles via the design of elliptical lattice [16]. However, the structure of the proposed elliptical lattice needs to be improved because the potential energy of the flock may not reach the minimum value when the velocity consensus is achieved. Another issue is that the orientation of the elliptical lattice does not align well with the lanes, which may cause vehicles not to move in the middle of lanes.

To solve the aforementioned problems, this letter proposes a novel elliptical lattice design and flocking control protocol by considering the heading direction of ground vehicles. The contributions of this letter are summarized as follows.

- A new elliptical lattice is developed for vehicle formations by non-trivally extending our previous work [16]. Six α-agents on one elliptical lattice are defined instead of four. The heading direction of an ellipse is aligned with the velocity direction of the ego α-agent instead of the γ-agent.
- 2) The orientation of the proposed elliptical lattice is defined and discussed for the first time. The Hamiltonian function of an elliptical lattice is analyzed, and it is concluded that in free space, the orientation cannot be controlled by the existing flocking theory [2].

2475-1456 © 2022 IEEE. Personal use is permitted, but republication/redistribution requires IEEE permission. See https://www.ieee.org/publications/rights/index.html for more information.

3) A novel interaction between α -agents and (permanent) road boundaries is defined, which serves as a penalty term to achieve the desired flocking lattice. Moreover, the relationship between the distance of lane boundaries and the length of the semi-minor axis is established to guarantee that the vehicle flock can move into the designed (numbers of) lanes or spaces.

The rest of this letter is organized as follows. Section II introduces preliminaries of flocking control and defines the elliptical flocking lattice. The new flocking control protocols for the proposed elliptical lattice are designed for free space and a bounded road in Section III. Section IV displays three simulation cases with different weights of $\alpha - \beta$ interactions. Finally, the conclusions are provided in Section V.

II. PRELIMINARIES AND ELLIPTICAL LATTICE DESIGN

In this section, the background of flocking control will be first introduced. Then, the desired elliptical lattice for multiagent ground vehicles by specifically considering practical ground traffic will be discussed.

A. Preliminaries of Flocking Control

The kinematic equation of N point-mass α -agents working on m dimensional Euclidean space is displayed in (1).

$$\begin{cases} \dot{q}_i = p_i \\ \dot{p}_i = u_i \end{cases} \quad i \in \mathcal{V}, \tag{1}$$

where q_i, p_i , and $u_i \in \mathbb{R}^m$ denote the position, velocity and control inputs of α -agent i, respectively. $\mathcal{V} = \{1, 2, \dots, N\}$. In this letter, α -agent j is called a neighbor of α -agent i if the condition $||q_j - q_i|| < r$ is satisfied, where r is the interaction range for α -agents, and $||\cdot||$ denotes the 2-norm operation. In addition, the $\sigma-norm$ defined in [2] is given by,

$$||z||_{\sigma} = \frac{1}{\epsilon} [\sqrt{1 + \epsilon ||z||^2} - 1]. \tag{2}$$

The control inputs for α -agent i in free space are defined by (3).

$$\begin{cases} u_{i} = u_{i}^{\alpha} + u_{i}^{\gamma}, \\ u_{i}^{\alpha} = c_{1}^{\alpha} \sum_{j \in N_{i}^{\alpha}} \phi_{\alpha}(\|q_{j} - q_{i}\|_{\sigma}) \mathbf{n}_{i,j} \\ + c_{2}^{\alpha} \sum_{j \in N_{i}^{\alpha}} a_{ij}(q)(p_{j} - p_{i}), \\ u_{i}^{\gamma} = c_{1}^{\gamma}(q_{\gamma} - q_{i}) + c_{2}^{\gamma}(p_{\gamma} - p_{i}). \end{cases}$$
(3)

where the u_i^{α} and u_i^{γ} represent $\alpha - \alpha$ and $\alpha - \gamma$ interactions, respectively. N_i^{α} is the set of spatial neighboring α -agents corresponding to α -agent i. $\mathbf{n}_{i,j} = (q_j - q_i)/\sqrt{1 + \epsilon \|q_j - q_i\|^2}$. $a_{ij}(q)$ is the element in a spatial adjacency matrix A(q) defined in [2]. The action function $\phi_{\alpha}(\cdot)$ is defined as,

$$\phi_{\alpha}(z) = \rho_{h}(z/\|r\|_{\sigma})\phi(z - \|d\|_{\sigma}), \tag{4}$$

where $\rho_h(\cdot)$ is a bump function, $\phi(\cdot)$ is an uneven sigmoidal function, and d denotes the desired lattice scale. The virtual γ -agent is commonly used to provide a virtual trajectory reference for α -agents (CAVs) path tracking. More details of flocking theory refer to [2], [8].

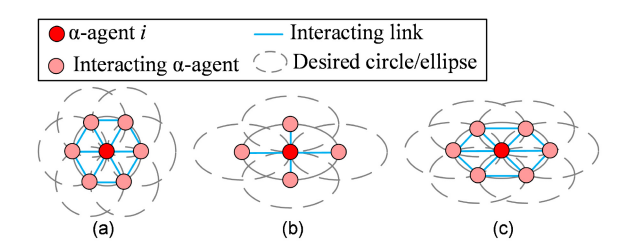


Fig. 1. (a) Flocking lattice in a circle with seven interacting α -agents. (b) Flocking lattice in an ellipse with five interacting α -agents. (c) Flocking lattice in an ellipse with seven interacting α -agents.

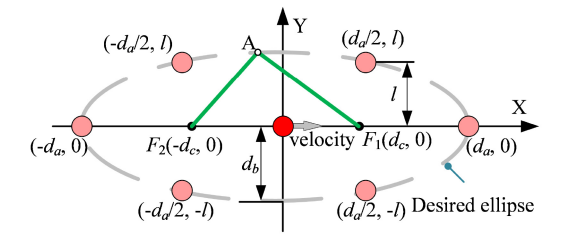


Fig. 2. A new elliptical flocking lattice with six interacting α -agents.

B. Elliptical Lattice for Multi-Agent Ground Vehicles

To achieve the desired formation of a flock, the lattice-type structure of α -agents was utilized in the literature [2], [7]. In this section, three different geometries of the flocking lattice, as shown in Fig. 1, will be investigated.

The first flocking lattice in Fig. 1(a) is achieved by employing the control protocol in (3). Due to the characteristic of the rigid or uniform interaction ranges and inter-agent gaps, this lattice was classified as a rigid spacing policy in [16]. Moreover, the distance difference between a pair of interacting α -agents and the constant lattice scale, d, is depicted in (5) using the σ – norm.

$$e_{ij} = \|q_j - q_i\|_{\sigma} - \|d\|_{\sigma}.$$
 (5)

Accordingly, the equation (4) with e_{ij} can be rewritten as,

$$\phi_{\alpha}(z, e_{ij}) = \rho_h(z/\|r\|_{\sigma})\phi(e_{ij}). \tag{6}$$

Fig. 1(b) shows an ellipse geometry for flocking lattice in [16]. Four neighboring agents of α -agent i are located on the semi-major and semi-minor axes of the desired ellipse. However, some practical issues of this pattern exist for flocking control of multi-agent ground vehicles. First, ground vehicles typically will not move side by side on the road, considering driving safety. Second, the potential energy does not reach the minimum value, which makes this pattern hard to be achieved.

To address the above issues, this letter proposed a new elliptical lattice, as shown in Fig. 1(c), where each ellipse is generally centered at one α -agent with six neighbors. The positions of these agents are displayed in Fig. 2. The coordinates of two α -agents on the semi-major axis are $(-d_a, 0)$ and $(d_a, 0)$, where d_a is the length of the semi-major axis. Let l be the lane width of a multi-lane road. The coordinates of the other four α -agents are $(d_a/2, l)$, $(-d_a/2, l)$, $(-d_a/2, -l)$, and $(d_a/2, -l)$. Apparently, the seven α -agents are designed to move along with three parallel lanes.

Next, the ellipse will be determined by calculating d_a and d_b (semi-minor axis). It is well-known that the summation of distances from any points on an ellipse to the two foci F_1 and F_2 always equals $2d_a$. Thus, the six neighboring α -agents on the ellipse satisfy the following equation,

$$||q_i - F_1|| + ||q_i - F_2|| = 2d_a.$$
 (7)

Substituting $q_j = (d_a/2, l)$, $F_1 = (d_c, 0)$, $F_2 = (-d_c, 0)$, and $d_c = \sqrt{d_a^2 - d_b^2}$ into (7), the semi-minor axis is calculated as,

$$d_b = \frac{2}{\sqrt{3}}l. (8)$$

Referring to equation (9) in [16], d_a is defined in (9).

$$d_a = t_h p_r + \mu_a, \tag{9}$$

where t_h denotes the time-headway, p_r is the velocity of the virtual leader, and μ_a is the minimum safety distance.

III. CONTROL DESIGN FOR ELLIPTICAL LATTICE

A. Control Design in Free Space

1) Calculation of Distance Errors: To calculate the control inputs for α -agents, the distance errors between neighboring α -agents and the desired interaction gap need to be determined. In [16], the distance error is formulated in (10).

$$\tilde{e}_{ii} = (\|q_i - F_1^i\| + \|q_i - F_2^i\|) - 2d_a, \tag{10}$$

where F_1^i and F_2^i are the two foci of the ellipse centered at q_i . Intuitively, $\tilde{e}_{ij} = \tilde{e}_{ji}$ may not be always satisfied. The orientation of each semi-major axis was assumed to be parallel to ensure $\tilde{e}_{ij} = \tilde{e}_{ji}$ in [16], which may not be practical.

In this letter, the semi-major axis is defined to be aligned with the velocity direction of the center α -agent. To ensure the interaction force between a pair of α -agents is the same, the distance error is finally determined by selecting the minimum value of the \tilde{e}_{ij} and \tilde{e}_{ji} , as shown in (11).

$$e_{ii} = e_{ii} = \min\{\tilde{e}_{ii}, \tilde{e}_{ii}\},\tag{11}$$

where \tilde{e}_{ij} and \tilde{e}_{ji} are rewritten by using the $\sigma-norm$,

$$\tilde{e}_{ij} = \frac{\|(\|q_j - F_1^i\| + \|q_j - F_2^i\|)\|_{\sigma}}{2} - \|d_a\|_{\sigma}, \quad (12a)$$

$$\tilde{e}_{ji} = \frac{\|(\|q_i - F_1^j\| + \|q_i - F_2^j\|)\|_{\sigma}}{2} - \|d_a\|_{\sigma}.$$
 (12b)

Therefore, the control protocol for the elliptical lattice in free space is defined in (13).

$$\begin{cases} u_{i} = u_{i}^{\alpha} + u_{i}^{\gamma}, \\ u_{i}^{\alpha} = c_{1}^{\alpha} \sum_{j \in N_{i}^{\alpha}} \phi_{\alpha}(\|q_{j} - q_{i}\|_{\sigma}, e_{ij}) \mathbf{n}_{i,j} \\ + c_{2}^{\alpha} \sum_{j \in N_{i}^{\alpha}} a_{ij}(q)(p_{j} - p_{i}), \\ u_{i}^{\gamma} = c_{1}^{\gamma}(q_{\gamma} - q_{i}) + c_{2}^{\gamma}(p_{\gamma} - p_{i}). \end{cases}$$

$$(13)$$

where the action function $\phi_{\alpha}(\|q_j - q_i\|_{\sigma}, e_{ij})$ is defined in (6) and e_{ij} is given by (11).

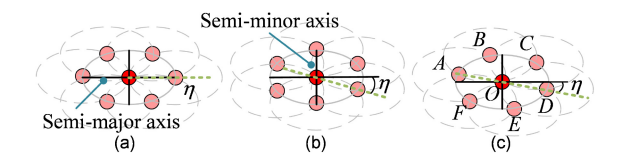


Fig. 3. (a) Desired ellipse with two α -agents on the semi-major axis. (b) Desired ellipse with two α -agents on the semi-minor axis. (c) Desired ellipse without α -agents on the axes.

2) Orientation of Flocking Lattice: Fig. 3 shows flocking lattices in three different orientations, with two neighboring α -agents on the semi-major or semi-minor axis, or none on the ellipse axes. To describe the orientation of the elliptical lattice, we first define the heading angle of the lattice, η .

Definition 1 (Heading Angle of the Elliptical Lattice): For the elliptical lattice, the heading angle is the angle between the desired velocity direction and the line connecting two α -agents on the ellipse with the longest distance.

According to this definition, the range of η is [0, $\tan^{-1}(d_b/(\sqrt{3}d_a))$], where the minimum and maximum cases are shown in Fig. 3(a) and Fig. 3(b), respectively.

Proposition 1: Via the $\alpha - \alpha$ interactions in (13), the maximum number of neighboring α -agents within the desired interaction distance on the proposed elliptical lattice is six, and they are centrosymmetric about the center of the ellipse.

Proof: Taking Fig. 3(c) as an example, α -agent $A(x_A, y_A)$ is on the ellipse centered on α -agent $O(x_O, y_O)$. Based on the geometric relationship, We have

$$\frac{(x_A - x_O)^2}{d_a^2} + \frac{(y_A - y_O)^2}{d_b^2} = 1.$$
 (14)

 α -agents $B(x_B, y_B)$ and $F(x_F, y_F)$ are on the two intersection points of the ellipses centered on α -agents A and O, respectively. Thus, α -agents B and F are simultaneously in the desired interaction distance of α -agents A and O. α -agent $C(x_C, y_C)$ is on another intersection point of the two ellipses centered on α -agents B and O, respectively (but does not interact with α -agents A and A). By utilizing (14) for different interacting A-agents (such A-agents A and A), A-agents A and A0, A-agents A1 and A2, seven pairs in total), A-agents A3 and A4 are obtained to be symmetric about A-agent A4 as shown in (15).

$$(x_C - x_O, y_C - y_O) = -(x_F - x_O, y_F - y_O).$$
 (15)

Similarly, we have symmetric paris,

$$(x_A - x_O, y_A - y_O) = -(x_D - x_O, y_D - y_O),$$
 (16a)

$$(x_B - x_O, y_B - y_O) = -(x_E - x_O, y_E - y_O).$$
 (16b)

Therefore, up to six neighboring α -agents are within the desired interaction distance on the proposed elliptical lattice. The average position of these α -agents is determined in (17).

$$\bar{q} = \frac{1}{7}(q_A + q_B + q_C + q_D + q_E + q_F + q_O) = q_O.$$
 (17)

To explore the rationale of three patterns in Fig. 3, we introduce a Hamiltonian function consisting of three parts, namely

the relative kinetic energy, the potential energy of $\alpha - \alpha$ agents, and the potential energy of $\alpha - \gamma$ agents.

$$\begin{cases}
H(q, p) = K(p) + V_{\alpha}(q) + V_{\gamma}(q), \\
K(p) = \frac{c_{2}^{\gamma}}{2} \sum_{i \in \mathcal{V}} \|p_{i} - p_{r}\|^{2}, \\
V_{\alpha}(q) = c_{1}^{\alpha} \sum_{i \in \mathcal{V}} \sum_{j \in \mathcal{V} \setminus \{i\}} \int_{\|d\|_{\sigma}}^{\|q_{j} - q_{i}\|_{\sigma}} \phi_{\alpha}(x) dx, \\
V_{\gamma}(q) = \frac{c_{1}^{\gamma}}{2} \sum_{i \in \mathcal{V}} \|q_{i} - q_{r}\|^{2}.
\end{cases} (18)$$

Proposition 2: Suppose the flocking lattice in Proposition 1 is formed, the Hamiltonian in (18) reaches the minimum value of $3c_1^{\gamma}(d_a^2+d_b^2)/2$ iff $q_r=\bar{q}$, and is independent of η .

Proof: The velocity consensus is achieved in steady state, and all neighboring α -agents are in the desired interaction distance. Therefore, K(p) = 0 and $V_{\alpha}(q) = 0$ are held. In this case, the Hamiltonian in (18) is

$$H(q, p) = V_{\gamma}(q) = \frac{c_1^{\gamma}}{2} \sum_{i \in \mathcal{V}} \|q_i - q_r\|^2.$$
 (19)

The derivation of H with respect to q_r is

$$\frac{dH(q_r)}{dq_r} = c_1^{\gamma} \sum_{i \in \mathcal{V}} (q_i - q_r). \tag{20}$$

The optimal solution q_r^* for the minima H^* is given as,

$$q_r^* = \frac{1}{N} \sum_{i \in \mathcal{V}} q_i = \bar{q} = q_O.$$
 (21)

Since α -agents B and F are on the intersection points of the two ellipses centered on α -agents A and O, respectively, it is easy to obtain that,

$$\|q_A - q_O\|^2 + \|q_B - q_O\|^2 + \|q_F - q_O\|^2 = \frac{3d_a^2 + 3d_b^2}{2}.$$
(22)

Substituting (15), (16), (21), (22) into (19), the minimum Hamiltonian, H^* , is derived as,

$$H^* = \frac{c_1^{\gamma}}{2} \sum_{i \in \mathcal{V}} \|q_i - q_r^*\|^2 = \frac{3c_1^{\gamma}}{2} \left(d_a^2 + d_b^2\right). \tag{23}$$

Eq. (23) indicates that the Hamiltonian function is independent of η . Thus, flocking control (13) obtained from minimizing the Hamiltonian function cannot control or adjust η .

B. Control Design in a Bounded Road

To apply the proposed elliptical lattice to regulate CAV driving on the road, permanent road (not lane) boundaries, which cannot be bypassed by CAVs and can interact with vehicles all the time, are investigated as β -agents to achieve the desired flocking orientation. Fig. 4 shows flocking with the proposed elliptical lattice in three patterns developed in Fig. 3. By appropriately selecting the interaction range and formulating the repulsive force of the road boundaries, the three elliptical patterns will converge to our dedicated pattern.

The repulsive forces of road boundaries with multiple lanes are defined in (24).

$$u_i^{\beta} = c_1^{\beta} f_w(\hat{q}_i - q_i) \hat{\mathbf{n}}_i + c_2^{\beta} \mathbf{1} (f_w(\hat{q}_i - q_i)) (\hat{p}_i - p_i), \quad (24)$$

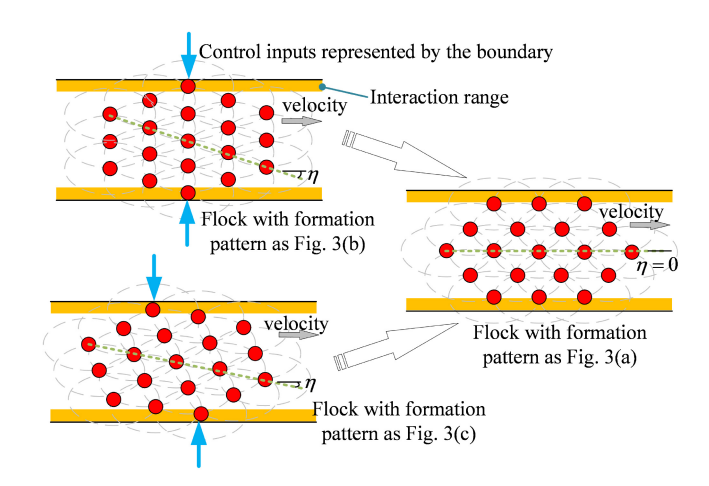


Fig. 4. Flocking with the proposed elliptical lattices interacting with permanent road boundaries.

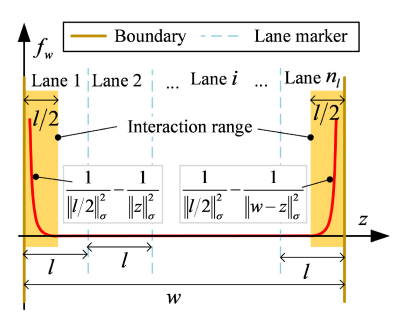


Fig. 5. An illustration of designed interaction forces from road boundaries (β -agents).

where the \hat{q}_i and \hat{p}_i are the position and the velocity of β_i agent [2]. $\hat{\mathbf{n}}_i = (\hat{q}_i - q_i)/\sqrt{1 + \epsilon \|\hat{q}_i - q_i\|^2}$. The indicator function, $\mathbf{1}(f_w(\hat{q}_i - q_i))$, is defined by $\mathbf{1}(f_w(\hat{q}_i - q_i)) = 1$ if $f_w(\hat{q}_i - q_i) > 0$, otherwise $\mathbf{1}(f_w(\hat{q}_i - q_i)) = 0$. Inspired from [1], the action function $f_w(x)$ is defined as,

$$f_w(x) = 1/\|l/2\|_{\sigma}^2 - 1/\|x\|_{\sigma}^2, 0 < x < l/2.$$
 (25)

Note that the action function in [1] was only focused on a single-lane driving scenario with limited applications, and cross-section artificial potential function in [13] was complicated. The repulsive forces of the road boundaries defined in this letter can be extended to any number of lanes with the specifically defined interaction range as follows.

An illustration of the repulsive forces from road boundaries is shown in Fig. 5, in which the interaction ranges are defined within the half lane width starting from the two (left and right) road boundaries. Let n_l be the number of lanes, $w = n_l l$ denote the distance between the two road boundaries.

Therefore, the flocking control protocol for elliptical lattices in a bounded road is defined as,

$$u_i = u_i^{\alpha} + u_i^{\beta} + u_i^{\gamma}. \tag{26}$$

where u_i^{α} and u_i^{γ} are given by (13), u_i^{β} is defined in (24).

IV. SIMULATION RESULTS AND DISCUSSIONS

In this section, the dynamics of twenty α -agents, tracking a virtual γ -agent, are investigated in free space and a bounded

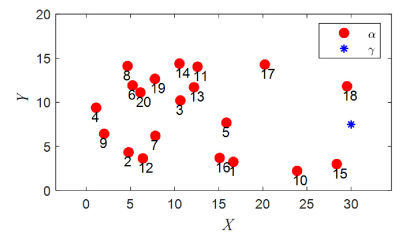


Fig. 6. The initial position of twenty α -agents and the (virtual) γ -agent.

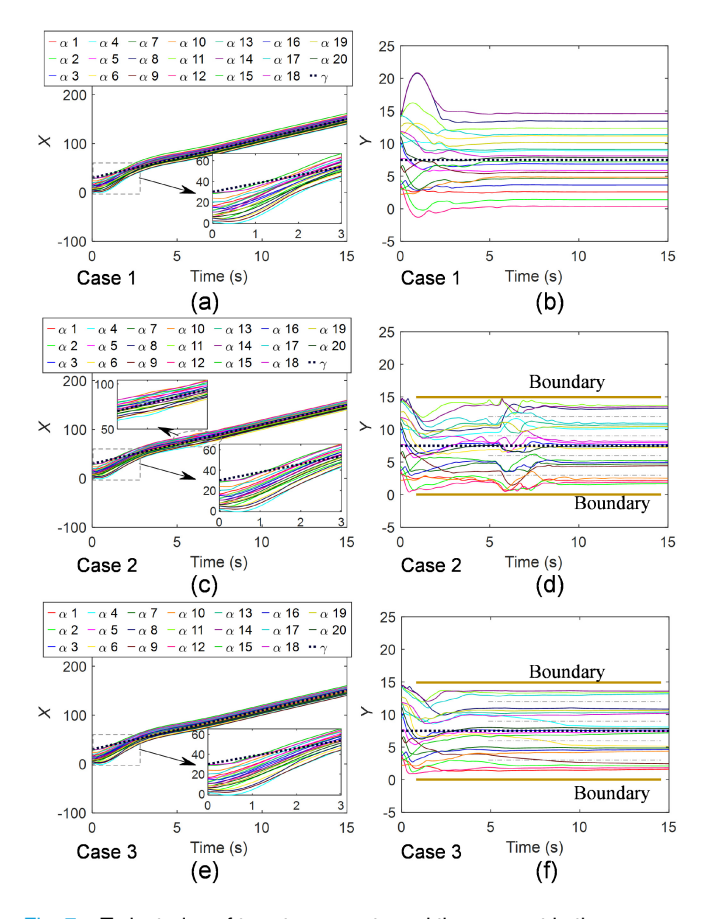


Fig. 7. Trajectories of twenty α -agents and the γ -agent in three cases.

road. The initial positions of the twenty α -agents are randomly determined in an area of [(0, 0), (30, 15)], and the γ agent is started at (30, 7.5), as shown in Fig. 6. The initial velocity of all α -agents is zero. Three simulation cases are analyzed with the same initialization conditions. In the first case (case 1), the flocking control protocol in (13) is employed to study the proposed elliptical flocking lattice in free space. In the second case (case 2) and the third case (case 3), the corresponding flocking control protocol in (26) is utilized with different c_1^{β} and c_2^{β} to analyze the influence of the boundaries' force in (24) on the flocking behavior. The parameters of this simulation are summarised in Table I.

Fig. 7 depicts the trajectories of all α -agents and the γ -agent in the X and Y directions for these three cases. As shown by the X direction trajectories in Fig. 7(a), Fig. 7(c), and Fig. 7(e), all α -agents in the three cases can approach the γ -agent at a same time. Fig. 7(b), Fig. 7(d), and Fig. 7(f) show the Y direction trajectories for the three cases. In case 1 of free space, the

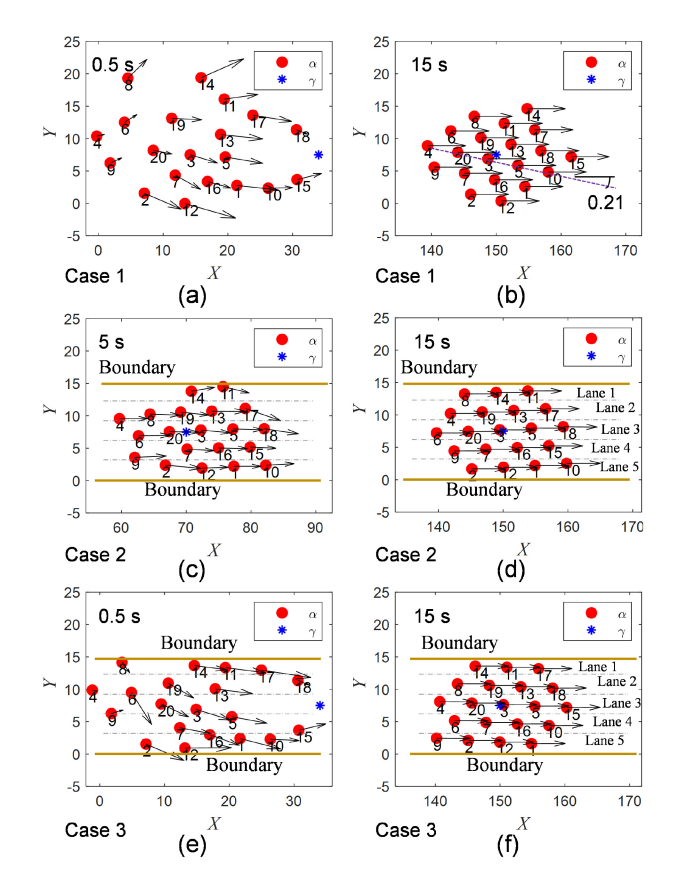


Fig. 8. Formation Pattern of twenty α -agents in three cases.

TABLE I
PARAMETER VALUES OF FLOCKING CONTROL

Symbol	Parameter values	Symbol	Parameter values
p_r	(8,0)	t_h	0.25
μ_a	3	w	15
n_l	5	l	3
d_a	5	d_b	$2\sqrt{3}$
ϵ	0.1	$\begin{vmatrix} d_b \\ r^{\alpha} \end{vmatrix}$	5.3
c_1^{α}	10	c_2^{α}	10
$c_1^{\beta}*$	[0,1.5,10]	$c_2^{\tilde{\beta}}*$	[0,1.5,10]
\hat{c}_1^{γ}	1	$ \tilde{c_2^{\gamma}} $	1

movement of α -agents first spread out and then stabilize in the range [-1.29, 20.84]. In case 2 and case 3, the two permanent boundaries are defined at Y = 0 and Y = 15, with five lanes. Due to the boundaries' effect given by (24), the movement of α -agents in the Y direction is in the range [0, 15]. Also, they can be divided into five lanes as expected.

Fig. 8 presents the result of flocking formation. The direction of the black arrow indicates the direction of the corresponding α -agent. The flocking lattice in the dedicated ellipse of a flock is formed. Furthermore, η in case 1 of free space is 0.21, as shown in Fig. 8(b), where η is 0 in case 2 and case 3 of a bounded road, as shown in Fig. 8(d) and Fig. 8(f). The formation results in Fig. 8(d) and Fig. 8(f) demonstrate that the method proposed in (26) can successfully form a flock with the dedicated flocking lattice in a bounded road.

Fig. 9 displays the velocity and control inputs for all α -agents in the three cases. As shown in Fig. 9(a), Fig. 9(e), and

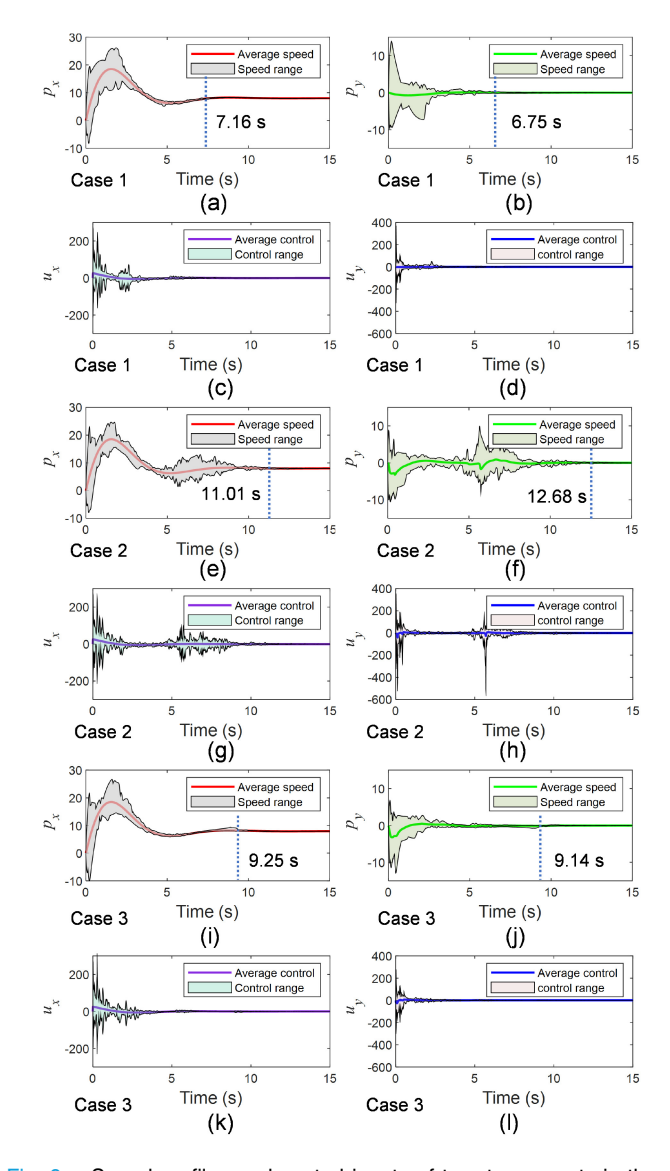


Fig. 9. Speed profiles and control inputs of twenty α -agents in three cases.

Fig. 9(i), the velocities of all α -agents in the X direction have a similar trend, where the time to reach the velocity match for case 1 is 7.16 s, which is faster than case 2 and case 3. Fig. 9(b), Fig. 9(f), and Fig. 9(j) show the velocity in the Y direction, where the matching time of case 1 is 6.75 s, which is still faster than the other two cases. The amplitude of control inputs in the X direction is similar for the three cases, as shown in Fig. 9(c), Fig. 9(g), and Fig. 9(k). The variation range of control inputs in the Y direction, as displayed in Fig. 9(d), Fig. 9(h), and Fig. 9(i), are different in the three cases. In case 3, the variation range is [-270.6, 246.9], which is smaller than that of case 1 and case 2. This indicates that a suitable weight of the $\alpha - \beta$ interactions can reduce the control inputs for the multi-agent systems. Motivated by the flocking navigation study of [17], the delayed and noisy response of α -agents will be investigated in the future.

V. CONCLUSION

This letter proposed a novel and elliptical lattice for regulating CAV motions on a bounded road by considering the heading direction, minimum safety distance, non-uniform longitudinal and lateral motions, and lane width. Two flocking algorithms were designed to achieve the elliptical flocking lattice in free space and bounded roads. Three simulation cases demonstrated the effectiveness of the proposed two algorithms, which have great potential to apply to CAV drivings and other multi-agent systems moving in non-uniform lattices.

REFERENCES

- [1] Y. Liu and B. Xu, "Improved protocols and stability analysis for multivehicle cooperative autonomous systems," *IEEE Trans. Intell. Transp. Syst.*, vol. 16, no. 5, pp. 2700–2710, Oct. 2015.
- [2] R. Olfati-Saber, "Flocking for multi-agent dynamic systems: Algorithms and theory," *IEEE Trans. Autom. Control*, vol. 51, no. 3, pp. 401–420, Mar. 2006.
- [3] F. Wang and Y. Chen, "A novel hierarchical flocking control framework for connected and automated vehicles," *IEEE Trans. Intell. Transp. Syst.*, vol. 22, no. 8, pp. 4801–4812, Aug. 2021.
- [4] C. W. Reynolds, "Flocks, herds and schools: A distributed behavioral model," SIGGRAPH Comput. Graph., vol. 21, no. 4, pp. 25–34, Aug. 1987.
- [5] J. Zhou, H. Qian, and X. Lu, "Multi-agent flocking via generalized control algorithms: Existence and properties," in *Proc. 14th Int. Conf. Control Autom. Robot. Vis. (ICARCV)*, 2016, pp. 1–6.
- [6] X. Zheng, T. Wang, S. Xue, J. Liu, H. Cao, and F. Hu, "Two-stage flocking formation control based on constrained boundary," in *Proc. 5th Chin. Conf. Swarm Intell. Cooper. Control*, 2021, pp. 1112–1122.
- [7] Z. Sun and B. Xu, "A flocking algorithm of multi-agent systems to optimize the configuration," in *Proc. China Autom. Congr. (CAC)*, 2021, pp. 7680–7684.
- [8] R. O. Saber and R. M. Murray, "Flocking with obstacle avoidance: Cooperation with limited communication in mobile networks," in *Proc.* 42nd IEEE Int. Conf. Decis. Control, vol. 2, 2003, pp. 2022–2028.
- [9] D. Huang, Q. Yuan, and X. Li, "Decentralized flocking of multi-agent system based on MPC with obstacle/collision avoidance," in *Proc. Chin. Control Conf. (CCC)*, 2019, pp. 5587–5592.
- [10] L. Iftekhar and R. Olfati-Saber, "Autonomous driving for vehicular networks with nonlinear dynamics," in *Proc. IEEE Intell. Veh. Symp.*, 2012, pp. 723–729.
- [11] H. Hu, S. Y. Yoon, and Z. Lin, "Flocking of wheeled vehicles in the presence of large communication delay through a potential functional approach," in *Proc. 52nd IEEE Conf. Decis. Control*, 2013, pp. 3529–3534.
- [12] F. Wang and Y. Chen, "Flocking control of multi-agent systems with permanent obstacles in strictly confined environments," *J. Auton. Veh.* Syst., vol. 1, no. 2, Sep. 2021, Art. no. 21005.
- [13] R. Hao, M. Liu, W. Ma, B. van Arem, and M. Wang, "A flock-like two-dimensional cooperative vehicle formation model based on potential functions," *Transportmetrica B, Transport Dyn.*, to be published.
- [14] C. F. Caruntu, C. Pascal, L. Ferariu, and C. R. Comsa, "Trajectory optimization through connected cooperative control for multiple-vehicle flocking," in *Proc. 28th Mediterr. Conf. Control Autom. (MED)*, 2020, pp. 915–920.
- [15] C. F. Caruntu, L. Ferariu, C. Pascal, N. Cleju, and C. R. Comsa, "Connected cooperative control for multiple-lane automated vehicle flocking on highway scenarios," in *Proc. 23rd Int. Conf. Syst. Theory Control Comput. (ICSTCC)*, 2019, pp. 791–796.
- [16] F. Wang, G. Wang, and Y. Chen, "Adaptive spacing policy design of flocking control for multi-agent vehicular systems," *IFAC-PapersOnLine*, vol. 55, no. 37, pp. 524–529, 2022. [Online]. Available: https://www. sciencedirect.com/science/article/pii/S2405896322028798
- [17] G. Vásárhelyi, C. Virágh, G. Somorjai, T. Nepusz, A. E. Eiben, and T. Vicsek, "Optimized flocking of autonomous drones in confined environments," *Sci. Robot.*, vol. 3, no. 20, p. eaat3536, 2018.